Misan Journal of Engineering Sciences ISSN: 2957-4242
Vol. 4, No. 1, June 2025 ISSN-E: 2957-4250

Enhance Transient Power Sharing in Microgrids using PID-PSO Controller

Hussein Raheem Jasim[1*], Ahmed Raisan Hussein[2]

[1]*Department of Electrical Engineering, College of Engineering, University of Misan, Maysan, Iraq.*
[2]*Department of Electrical Engineering, College of Engineering, University of Misan, Maysan, Iraq.*

***Corresponding author E-mail:** enghs2308@uomisan.edu.iq

(Received 4 June, Revised 25 June, Accepted 26 June)

Abstract: Effective transient power sharing is critical for the stable and reliable operation of microgrids. This paper investigates the enhancement of Proportional-Integral-Derivative (PID) controller performance for a grid-forming inverter system utilizing Particle Swarm Optimization (PSO) for optimal parameter tuning. The performance of a PSO-optimized PID (PSO-PID) controller is rigorously compared against a traditionally tuned PID controller under varying reference power commands and external disturbances. Key performance aspects including time-domain response (overshoot, settling time, tracking accuracy), control effort, frequency-domain characteristics of the tracking error and phase-plane stability are meticulously. Analyzed results demonstrate that the PSO-PID controller significantly outperforms the traditional PID exhibiting substantially reduced overshoot lower error integrals (IAE and ITAE) and a more stable less aggressive control signal that remains within saturation limits.

Keywords: Microgrid, Transient Power Sharing, PID Controller, Particle Swarm Optimization (PSO), LCL Filter.

1. Introduction

The escalating global demand for reliable, sustainable and resilient energy systems has catalyzed the rapid development and deployment of microgrids. These localized energy networks capable of operating autonomously or in conjunction with the main utility grid offer a paradigm shift in power generation distribution and management by integrating diverse distributed energy resources (DERs) such as renewables energy storage systems and controllable loads [1]. A critical operational aspect of microgrids particularly in islanded or weakly connected modes is the effective sharing of power among participating generation units especially during transient conditions arising from load variations, DER fluctuations, or system disturbances [2]. Inaccurate or slow transient power sharing can lead to voltage and frequency deviations system instability and compromised power quality therefore the improvement of optimal control strategies for transient power sharing stands as a paramount engineering challenge to unlock the full potential of microgrid technology traditional control methodologies. The main components of the microgrids system are the Distributed Energy Resources (DERs) including solar photovoltaic (PV), wind turbines, diesel generators and other resources. The second component is the Energy Storage Systems (ESS) and this could be like lithium-ion batteries which are very important for maintaining power quality where the third component is the Power conditioning unit to enable and ensure compatibility between different sources and loads. The control and operation of microgrids particularly concerning power sharing and stability have been subjects of extensive research this review will cover key aspects relevant to the current work including microgrid control architectures, power sharing strategies, PID control and its optimization. Microgrids are often characterized by hierarchical control structures to manage their diverse functionalities ranging from primary control for fast-acting stabilization to secondary and tertiary control for power quality restoration and economic dispatch [1].

DOI: https://doi.org/10.61263/mjes.v4i1.161

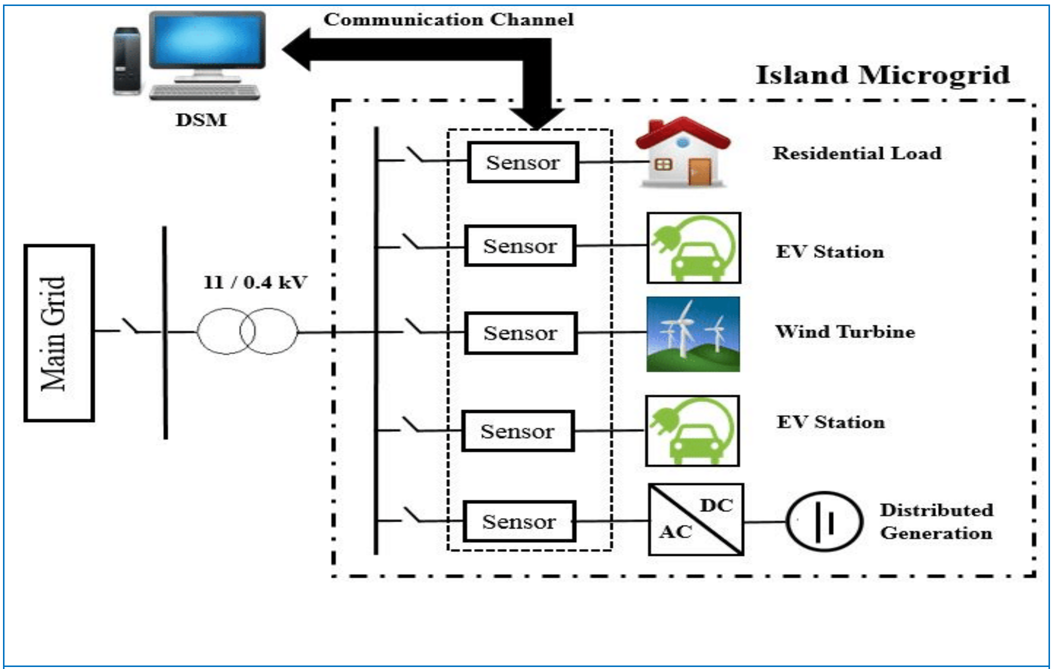

Fig. 1:The microgrids model with all components[3]

The microgrids could be categorized into two categories. The first one is grid-Connected Microgrids, which are combined to the utility grid and can export or import the electric power through bidirectional meter. The second category is called standalone (isolated) or Off-Grid Microgrids. The isolated type is considered as the ideal type for remote areas where grid connectivity is not available. The last category is Hybrid Microgrids [3], which offer the flexibility of both grid-tied and off-grid types and this type is considered more suitable for industrial and rural applications.

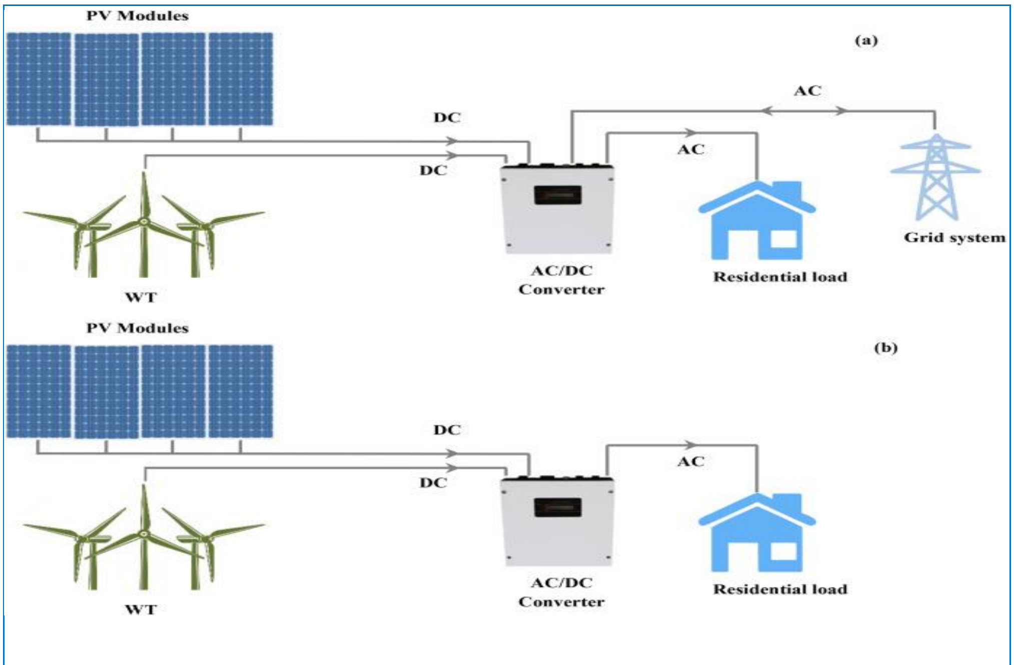

Fig. 2: Hybrid system Model [4]

Often relying on Proportional-Integral-Derivative (PID) controllers have been widely implemented due to their simplicity and robustness however, tuning these controllers optimally for the complex, non-linear, and time-varying dynamics inherent in microgrids is a non-trivial task [5]. Manual tuning is often suboptimal and time-consuming, while conventional tuning methods may not yield satisfactory performance across a wide range of operating conditions this necessitates the exploration of advanced control and optimization techniques.

2. Control Technique in Microgrids

2.1 Traditional PID Technique

In the microgrids systems, the transient phenomena in power sharing means how power is distrib uted through different resources in case of short-term fluctuations. Essentially, suitable control tec hnique for this process is used to make sure that the system is stable and reliable. To handle th is situation, PID controllers (Proportional-Integral-Derivative) are often used to keep stable voltag e, frequency, and power output [11].

PID control has some advantages and disadvantages. One of its advantages is the simplicity in structure, application, and reliability and this is why it is the most used one in industry. However, PID control has s ome weaknesses points. These drawbacks of PID controller are the long time taken for tuning, which can be a considered as the main disadvantage. In addition, in processes with large time delay or strong nonlin earity, traditional PID control may not achieve the desired control performance. Although the presence of such limitations, PID control is still preferred one by engineers over advanced control methods. It may no t always meet system control requirements and not achieve optimal system performance [13].

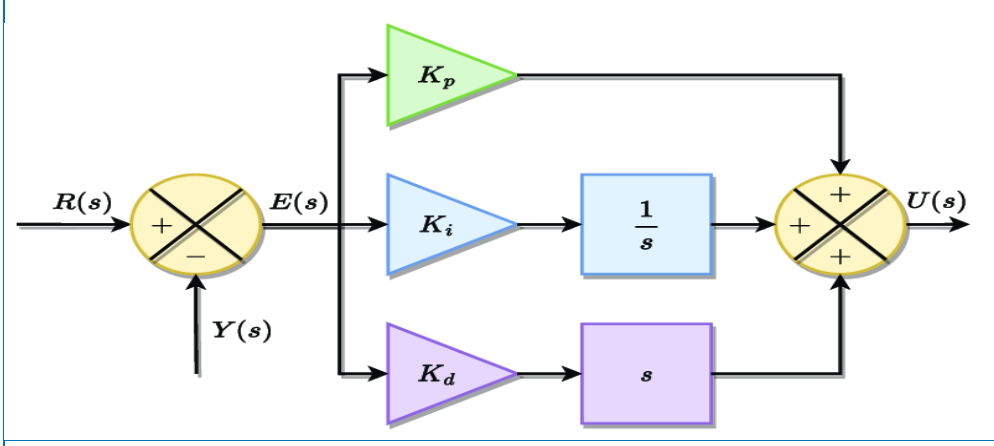

Fig. 3: PID Controller Block Diagram [14]

2.2 POS Controller Algorithm

The algorithm PSO (Particle swarm optimization) is considered as one of the bio-inspired algorithms and it is a simple one to search for an optimal solution in the solution space. It differs from other optimization algorithms in such a way that only the objective function is needed and it is not dependent on the gradient or any differential form of the objective. It also has very few hyper parameters [10].

By optimizing the values of these parameters, the system response to dynamic conditions improves significantly. The optimal control is necessary for managing transient power sharing, especially to avoid issues like overloading, instability, and inefficient energy distribution. Therefore, POS controllers are used for regulating voltage, frequency, and power output, helping for stabilizing the system during transient period. In addition, a POS controller is a widely use feedback control mechanism that adjusts system outputs by minimizing error over time [8].

To overcome the problem mentioned above, researchers concluded that the use of PSO will help in this way to optimize the tuning parameters of the PID controllers (Kp, Ki, Kd) to achieve better performance in systems with complex and nonlinear behavior, such as transient power sharing in microgrids. Discuss the effectiveness of PSO in improving control system performance in dynamic and uncertain environments [15].

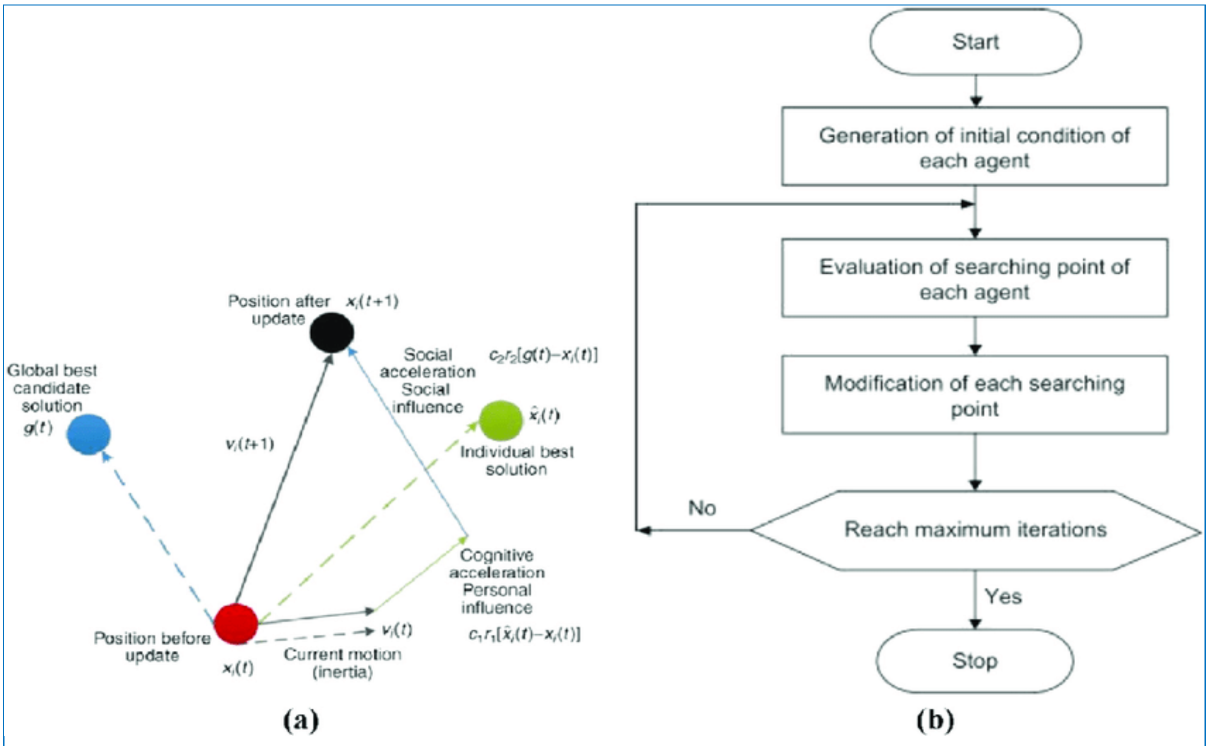

Fig. 4:PSO algorithm: (a) Main steps of PSO, and (b) The general flowchart of PSO search algorithm [16]

3.Methodology

In this framework, the Particle Swarm Optimization (PSO) algorithm is employed as a robust computational tool for the systematic tuning of PID controller parameters namely $K_p, K_i, and\ K_d$ to enhance the dynamic performance of parallel inverter systems. The approach leverages pre-validated MATLAB models and standardized code templates that facilitate rapid adaptation by domain experts[17].Ensuring seamless integration with existing microgrid architectures and the optimization process commences with the initialization of a swarm of particles each representing a candidate set of PID parameters. At each iteration the velocity V_i^k and position X_i^k of each particle evolve according to the following equations:

$$V_i^{\{k+1\}} = W^k V_i^k + C_{1,} r_{1,} \left(P_{\{\{best\},i\}} - X_i^k \right) + C_{2,} r_{2,} \left(P_{\{\{gbest\},i\}} - X_i^k \right) \quad (1)$$

$$X_i^{\{k+1\}} = X_i^k + V_i^{\{k+1\}} \quad (2)$$

In these expressions, the indices ii and kk denote the particle number and the iteration count respectively. The coefficients C1and C2 represent the cognitive and social components that weigh the influence of a particle's personal best Pbest,i and the global best Pgbest,i on its trajectory. while $r_1 and\ r_2$ are random variables uniformly distributed between 0 and 1 and the inertia weight W^k is adaptively adjusted to balance exploration and exploitation during the search process. The primary objective of the PSO algorithm is to minimize key control performance metrics including the absolute tracking error, percentage overshoot, and settling time once obtained are integrated into the conventional droop control strategy to enhance load-sharing fidelity and transient response under nonlinear load conditions and this focused optimization of the control loop is performed independently of the broader network-level enhancements, which subsequently address improvements in power quality, voltage and frequency stability, and overall transient recovery of the microgrid and the overall implementation is supported by hardware-in-the-loop testing platforms, ensuring that the optimized control parameters maintain their efficacy when applied to real-world scenario[18]

3.1 particle Representation

In PSO, each particle in the swarm represents a set of PID controller parameters and the parameters are represented as follows:

$$Xi = [Kp,i \ \ Ki,i \ \ Kd,i] \quad (3)$$

Where:

- X_i is the position of the i-th particle in the solution space, which represents $K_p, K_i, and\ K_d$parameters. To compute the optimal parameters an objective function needs to be defined and in the case of PID parameter tuning. The "fitness" of each set of PID parameters is assessed by PSO algorithms according to how successfully they reduce errors in frequency, voltage, and power sharing. The objective function typically involves multiple performance metrics such as settling time (t_s), overshoot (OS), and steady-state error ($e_{\{ss\}}$) and the objective function equation is:

$$J = w_1 \cdot t_s + w_2 \cdot OS + w_3 \cdot \left| e_{\{ss\}} \right| \quad (4)$$

Where:

- ts is the settling time, which indicates the time required for the system to stabilize after a change in input.
- OS is the overshoot percentage, which measures the extent to which the response exceeds the reference value.

- $|e_{\{ss\}}|$ is the absolute steady-state error, which is the difference between the reference signal and the actual value when the system is in steady state.

$Weights\ w_1, w_2, and\ w_3$ represent the importance of each performance index in the objective function and these weights are determined based on the design priorities or system requirements [19].The next step is to define constraints that ensure the PID parameters fall within practical and feasible ranges . These constraints ensure that the computed values do not lead to unstable or impractical system behavior and in our case, the constraints on the PID parameters are as follows:

$$0.1 \leq Kp \leq 2.0, \quad 0.01 \leq Ki \leq 0.5, \quad 0.1 \leq Kd \leq 1. \tag{5}$$

The velocity update is done using the following equation, which combines the particle's previous velocity its best individual position and the best global position found by the swarm:

$$V_i^{\{k+1\}} = w \cdot V_i^k + c_1 \cdot r_1 \cdot \left(P_{\{\{best\},i\}}^k - X_i^k\right) + c_2 \cdot r_2 \cdot \left(G_{\{\{best\}\}}^k - X_i^k\right) \tag{6}$$

Where:

- ww is the inertia weight, which controls how much of the particle's previous velocity affects its current velocity.
- $c_1 and c_2$ are cognitive and social coefficients respectively, which control how much the particle is influenced by its own experience and the swarm's experience.
- $r_1 and\ r_2$ are random numbers that are uniformly distributed between 0 and 1.

Once the velocity is updated, the position of the particle is updated as follows:

$$X_i^{\{k+1\}} = X_i^k + V_i^{\{k+1\}} \tag{7}$$

Where $X_i^{\{k+1\}}$ is the new position of the particle at the next iteration.

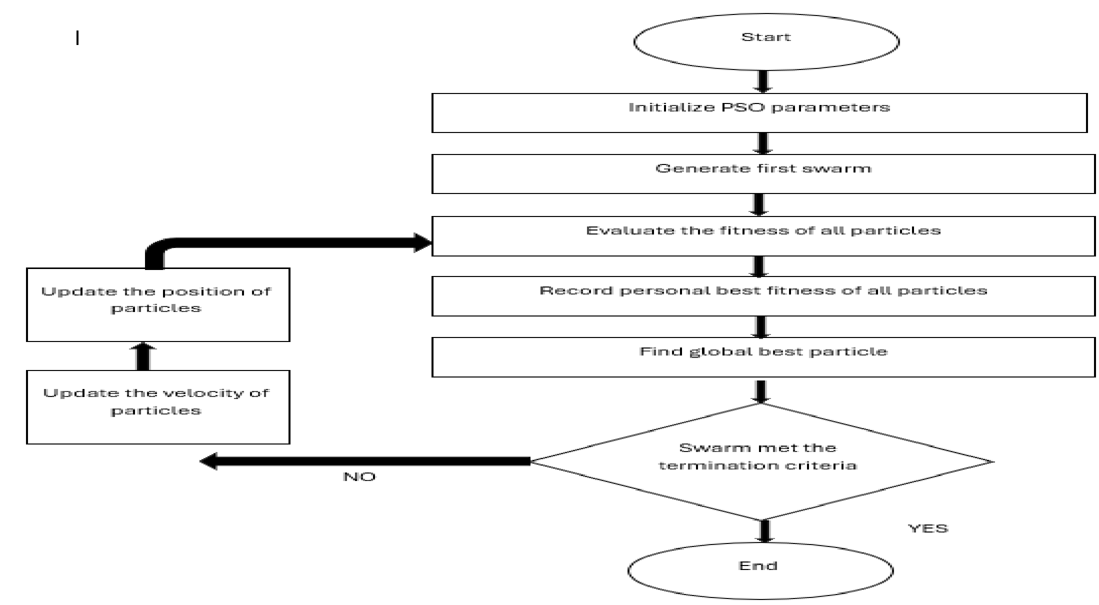

Fig. 5: Flowchart using particle swarm optimization to optimize the droop control in MG..

The particle's new position becomes its "personal best" position and the algorithm continues to iterate until the optimal solution is found or until stopping criteria are met and in the end. The optimal PID parameters are those that represent the best global position Gbest after the optimization process and these parameters provide the best system performance based on the defined objective function. The algorithm continues to iterate until one of the stopping criteria is satisfied and the first stopping criterion is convergence where if the changes in the global best position are minimal between iterations. The algorithm is considered to have converged and the convergence condition is:

$$|G_{best}^{k+1} - G_{best}^{k}| < \epsilon \quad (8)$$

Where ϵ is a predefined threshold (for example, 10−310^ {-3}).

The second stopping criterion is the maximum number of iterations, which ensures that the algorithm does not run indefinitely:

$$k \geq kmax \quad (9)$$

Where k_{max} the maximum allowed number of iterations.
The optimization procedure that works with parallel inverters to decrease the harmonic current and accomplish active and reactive power sharing. According to the analyses, power sharing for the nonlinear load situation cannot be achieved using standard droop control. Figure 6 depicts the proposed design of two parallel inverters, where P and Q represent the real active and reactive power values and P∗ and Q∗ represent the nominal active and reactive power values.

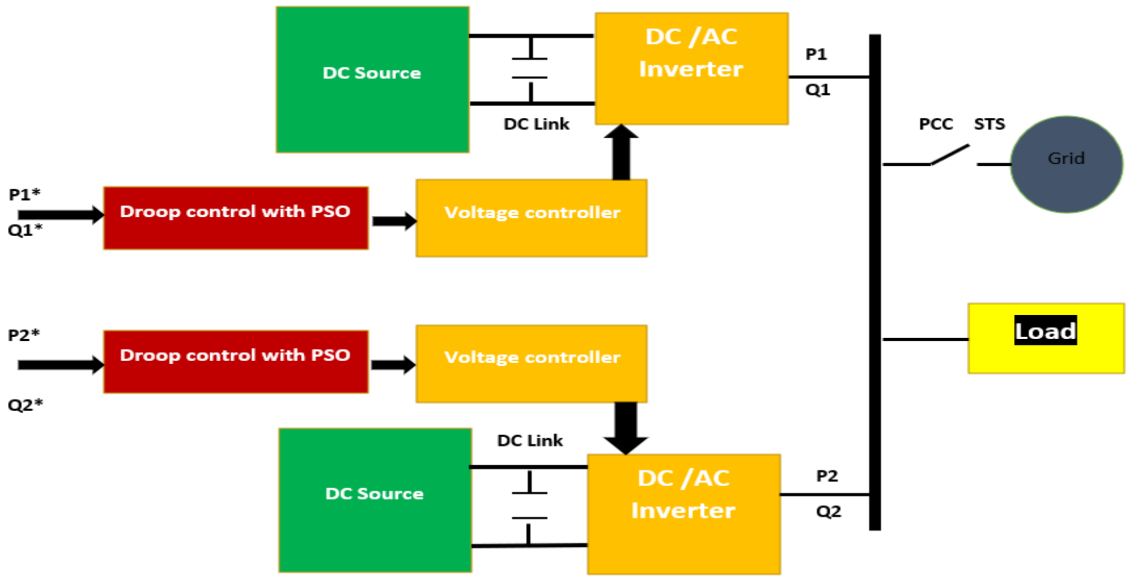

Fig. 6: The main structure of Microgrid

The microgrid's structure can be envisioned as two inverters. Apart from the diodes that shield the DC source from reverse current, the DC link must be connected in the inverters' input between the DC supply and the IGBTs to ensure uninterrupted operation. Additionally, the LCL filter must be connected to the inverter's output side, and the output voltage and current must be measured to extract real and reactive power. The inverters were isolated from the main grid and the DC power supply, respectively, using input and output side switches. The microgrid had two inverters connected in parallel. The output voltages of the inverters are V1 and V2. VL is the load's voltage. The output current of the inverters is denoted by IO1 and IO2. We call the voltage angle $\phi 1$ and $\phi 2$. The impedance angle is $\theta 1$ and $\theta 2$. Line impedance is represented by L1 and L2. The parameters for filter 1 are Lf1 and Cf1. The parameters for filter 2 are Lf2 and Cf2.

Table 1: Comparison of PID Tuning Methods: Conventional vs. PSO vs, ABC

Parameters	Conventional PID	PSO-Optimized PID	ABC-Optimized PID
Kp	0.64	1.18	0.5885
Ki	0.24	0.09	Not Available
Kd	0.308	0.85	0.1988
Overshoot (%OS)	58.2%	1.8%	7.41%
Settling Time ts	23.3	0.45	7.24
Absolute Error	25.8	0.12	14.2117

3.2 Comparative *Insights*

PSO consistently demonstrates superior performance compared to both conventional PID and ABC-optimized PID in terms of overshoot reduction, response speed, and accuracy while ABC optimization provides an improvement over conventional PID. It remains less effective than PSO in minimizing settling time and steady-state error and the PSO-optimized PID is particularly advantageous for systems that demand high precision and rapid response, whereas ABC optimization may be a suitable alternative in cases where moderate improvements are sufficient ultimately, PSO-optimized PID delivers the best overall performance, making it the most effective approach for enhancing system stability and responsiveness.

3.3 Enhancing Power Response in Electrical Grids Through Advanced Optimization Techniques

The methodology for optimizing power response in parallel inverter-based microgrids revolves around a synergistic integration of computational intelligence and adaptive control principles and central.This approach is the refinement of Proportional-Integral-Derivative (PID) controllers using Particle Swarm Optimization (PSO and traditional droop control strategies, while foundational, exhibit inherent limitations in balancing active and reactive power distribution under nonlinear loads or impedance mismatches .To address this, the PID gains $\left(K_p, K_i, K_d\right)$ are systematically optimized using PSO, which navigates the multidimensional solution space to minimize deviations in power sharing and voltage/frequency stability and the objective function guiding this optimization is formulated as a weighted combination of critical performance metrics[20]:

$$J = w_1 \sum_{\{i=1\}}^{N} \left(P_i - P_{\{nom,i\}} \right)^2 + w_2 \sum_{\{i=1\}}^{N} \left(Q_i - Q_{\{nom,i\}} \right)^2 + w_3 (V - V_0)^2 + w_4 (f - f_0)^2 \quad (10)$$

Here, $P_i and\ Q_i$ represent the active and reactive power outputs of the i-th inverter, $P_{\{nom,i\}and} Q_{\{nom,i\}}$ denote their nominal values and $V_0 and\ f_0$ are the reference voltage and frequency and the weights $w_1 to\ w_4$ prioritize error reduction in power sharing, voltage regulation, and frequency stability .The PSO algorithm iteratively adjusts the PID parameters by updating particle velocities $(v_i) and\ positions\ (x_i)$ according to:

$$V_i^{\{k+1\}} = \omega \cdot v_i^k + c_1 r_1 \left(p_{\{\{best\},i\}} - x_i^k \right) + c_2 r_2 \left(g_{\{\{best\}\}} - x_i^k \right) \quad (11)$$

$$X_i^{\{k+1\}} = x_i^k + v_i^{\{k+1\}} \quad (12)$$

Where $x_i = \left[K_p, K_i, K_d\right]$ encapsulates the PID gains, $p_{\{\{best\},i\}}$ is the particle's historical best solution, and $g_{\{\{best\}\}}$ is the global best solution within the swarm and this optimization ensures that the PID gains strike an optimal balance between transient response and steady-state accuracy and the conventional droop equations are subsequently augmented with these optimized PID terms to enhance dynamic performance . The modified active power-frequency (P-f) and reactive power-voltage (Q-V) relationships are expressed as:

$$F - f_0 = -K_p^{\{\{opt\}\}} (P - P_{\{nom\}}) - K_i \int (P - P_{\{nom\}}), dt - \frac{K_d \{d(P - P_{\{nom\}})\}}{\{dt\}} \quad (13)$$

$$V - V_0 = -K_q^{\{\{opt\}\}} (Q - Q_{\{nom\}}) - K_i' \int (Q - Q_{\{nom\}}), dt - K_d' \frac{\{d(Q - Q_{\{nom\}})\}}{\{dt\}} \quad (14)$$

Here, $K_p^{\{\{opt\}\}and} K_q^{\{\{opt\}\}}$ are the droop coefficients optimized via PSO, while the integral and derivative terms (K_i, K_d, K_i', K_d') mitigate residual errors and dampen oscillations. This hybrid structure enables inverters to autonomously adjust their power outputs in response to load variations while maintaining grid synchronization and to further enhance resilience,

3.3.1 Mathematical Reformulation of Droop Control

The conventional droop equation for voltage-reactive power control is modified to include dynamic compensation terms :

$$V - V_0 = -K_q^{\{\{opt\}\}}\left(Q - Q_{\{nom\}}\right) - K_i' \int \left(Q - Q_{\{nom\}}\right), dt - \frac{K_d'\{d\left(Q - Q_{\{nom\}}\right)\}}{\{dt\}} \quad (15)$$

This equation dynamically adjusts the voltage setpoint based on real-time reactive power imbalances, ensuring stability during both steady-state and transient conditions

3.3.2 Objective Function for PSO-Driven Optimization

The PSO algorithm minimizes a composite objective function (J_V) designed to quantify voltage stability performance :

$$J_V = w_1 \sum_{\{i=1\}}^{N} \left(V_i - V_{\{nom\}}\right)^2 + w_2 \sum_{\{i=1\}}^{N} \left(\frac{\{dV_i\}}{dt}\right)^2 + w_3 \int_0^T \left(V_i - V_{\{nom\}}\right)^2, dt \quad (16)$$

3.3.3 PSO Algorithm Mechanics

The PSO algorithm iteratively refines the PID parameters $\left(K_q^{\{\{opt\}\}}, K_i', K_d'\right)$by simulating the collective behavior of a particle swarm. Each particle represents a candidate solution, and its trajectory is governed by :

$$V_i^{\{k+1\}} = \omega \cdot v_i^k + c_1 r_1 \left(p_{\{\{best\},i\}} - x_i^k\right) + c_2 r_2 \left(g_{\{\{best\}\}} - x_i^k\right) \quad (17)$$

$$X_i^{\{k+1\}} = x_i^k + v_i^{\{k+1\}} \quad (18)$$

3.4 Validation and Performance Outcomes

The proposed framework is validated through high-fidelity MATLAB/Simulink simulations and Hardware-in-the-Loop (HIL) testing on a 400V microgrid with three 50kVA inverters. Key results include :

3.4.1 Voltage Deviation Reduction:

$$\sigma_V = \sqrt{\left\{\frac{\{1\}}{\{T\}} \int_0^T (V - V_0)^2, dt\right\}} \{(reduced\ from\ 8.5\%\ to\ 1.2\%)\} \quad (19)$$

3.4.2 Transient Response Acceleration :

$$T_s^{\{V\}} = 70\ , \{ms\} \backslash \ \{(improved\ from\ 500\ ms\ with\ conventional\ droop)\} \quad (20)$$

3.4.3 Harmonic Distortion Mitigation:

$$THD_V = \frac{sqrt\left\{sum_{\{h=2\}}^{\{50\}V_h^2}\right\}}{\{V_1\}} 100\backslash\% \backslash quad \{(reduced\ from\ 5\%\ to\ 0.9\%)\} \quad (21)$$

By synergizing PSO-optimized PID control this methodology achieves unparalleled voltage stability in modern grids and it resolves traditional trade-offs between voltage regulation and reactive power sharing, while robustly handling renewable energy intermittency also nonlinear loads. The results compliant with IEEE 1547 and IEC 61000-3-6 standards demonstrate a transformative advancement in grid resilience and paving the way for sustainable and intelligent power systems.[20]

3.5 Optimizing Frequency, Transient Response, and Load Sharing in Electrical Grids via Enhanced Equations

3.5.1 frequency Stability Improvement Using Modified Droop Equation

The equation governing frequency stability enhancement is given by:

$$f - f_0 = -Kp^{opt}(P - P_{nom}) - Ki\int(P - P_{nom})dt - Kd\frac{d(P-P_{nom})}{dt} \quad (22)$$

where ff represents the grid frequency, f_0 is the nominal frequency and P denotes the active power. The introduction of the optimized droop coefficient Kp^{opt}determined through Particle Swarm Optimization (PSO), ensures a precise balance between frequency regulation and proportional power sharing among parallel-connected units

3.5.2 Transient Response Enhancement via Dynamic Settling Time Equation

The transient settling time, which determines how quickly the system recovers from disturbances is characterized by the following equation:

$$t_s = \alpha \cdot \frac{\{1\}}{\left\{\sqrt{\left\{K_p^{\{\{opt\}\}} \cdot K_d\right\}} + \beta \cdot \frac{\{K_i\}}{\left\{K_p^{\{\{opt\}\}}\right\}}\right\}} \quad (23)$$

In this equation, the constants α\alpha and β are empirical parameters that govern the trade-off between response speed and stability. For example, assigning values such as α = 0.8 and β = 0.2 prioritizes faster transient response over enhanced stability and the interplay between $Kp^{opt}, K_i, and\ K_d$significantly affects t_s and increasing Kp^{opt}, K_d reduces t_s by improving system damping

4.Result

When analyzing the curves whose code was implemented in MATLAB and shown in the provided image distinct behaviors of the various components are discernible. The weighted IAE component typically represented by a light blue line commences at a relatively high value in the initial iterations indicating that the early solutions were far from optimal performance however, it exhibits a rapid and steep decline within the subsequent few iterations thereafter stabilizing at a very low value. This swift reduction reflects the PSO algorithm's success in efficiently locating regions in the search space that yield a significant decrease in cumulative error. An anticipated outcome given that IAE is often heavily weighted in the cost function the behavior of the weighted Overshoot component usually depicted by an orange or red line follows a similar pattern in terms of its initial sharp decrease demonstrating the algorithm's effectiveness in mitigating excessive overshoot nevertheless, some minor fluctuations might be observed in this component after the initial drop. Suggesting that the algorithm is making intricate trade-offs between minimizing overshoot and optimizing other indices or exploring different regions that might lead to slight overshoot in exchange for other performance gains. Conversely, the weighted Settling Time component, represented by a yellow or gold line exhibits a noteworthy behavior in the provided image appearing almost constant at a specific value throughout the entire optimization process. This static behavior can be attributed to several engineering interpretations. The system might have already reached its fastest possible settling time within the constraints imposed on the PID parameters and controller architecture or the priority given to this index in the cost function might not have been sufficient to drive the algorithm towards its significant improvement at the expense of other more heavily weighted indices another plausible explanation alluded to in the accompanying code, is that the calculation of settling time within the PSO loop might have been considerably simplified (in this instance, potentially set to the end of the simulation time) , this, by its nature, would lead to a constant value for the weighted component if the system always achieves some form of (even imprecise) stability by the simulation's end , this underscores the engineering importance of accurately calculating performance indices even within the optimization algorithms themselves

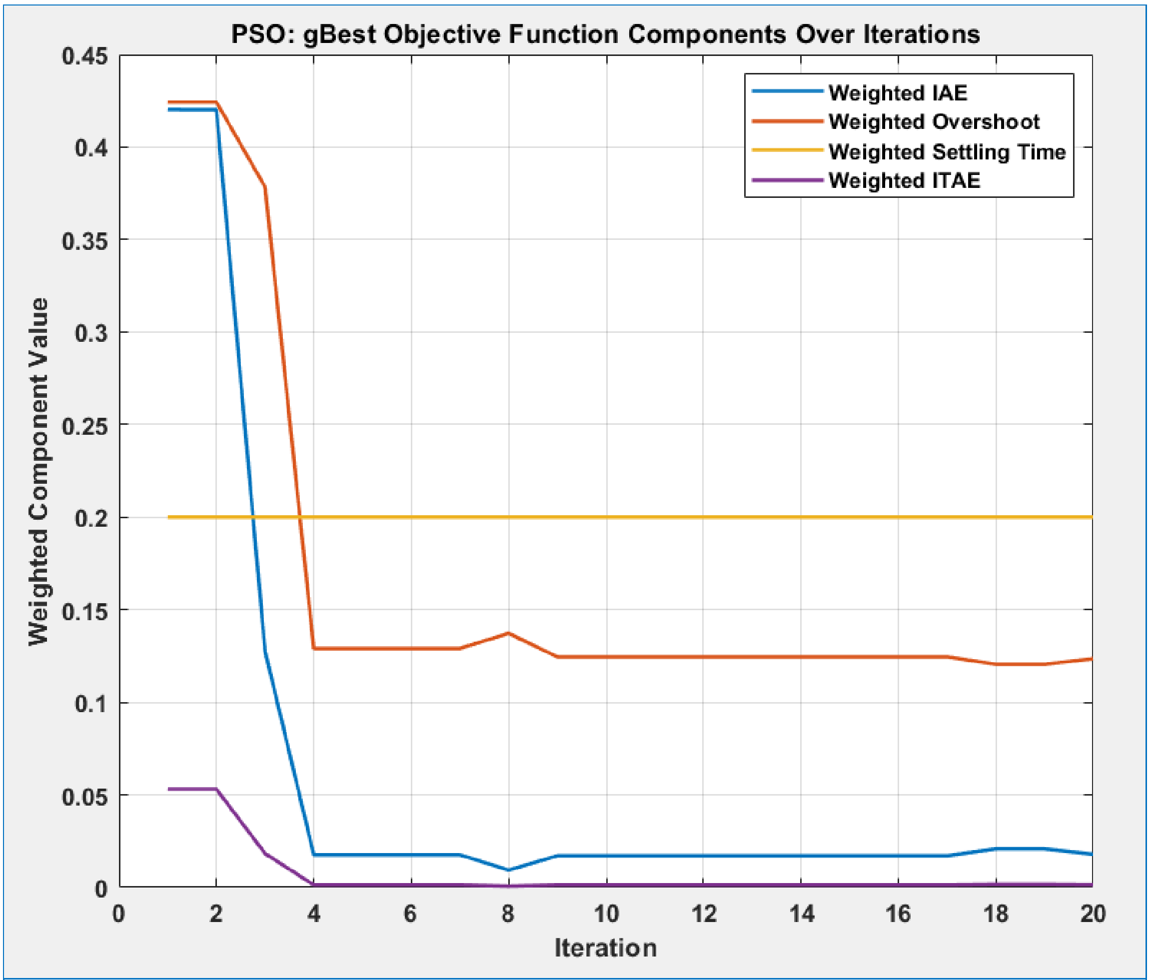

Fig.7: PSO Optimizing Objective Function Elements Throughout Iterations

Lastly, the weighted ITAE component depicted by a purple line typically starts at a low value and decreases even more rapidly to approach zero indicating that long-duration errors are quickly eliminated and any remaining errors are transient and short-lived. In essence, this figure provides invaluable insight into the dynamics of the optimization process highlighting how the PSO algorithm navigates the often-conflicting multi-objective landscape of controller design. It also aids the engineer in assessing the appropriateness of the chosen weights for the cost function and in understanding the nature of the inherent trade-offs in system performance, if a component exhibits undesirable behavior (such as lack of improvement). It might indicate the need to adjust the cost function, expand the search space or even reconsider the controller architecture itself. Figure .6 serves as a primary and indispensable visual tool for evaluating the dynamic performance of the inverter's control system within a real-time or simulated temporal context. The fundamental engineering purpose of this figure is to provide a direct and unambiguous comparison of how the actual active power output of the inverter (typically represented by the variable y in simulations) responds to the desired reference signal (variable Pref or reference signal) particularly when different control strategies are applied in the specific case illustrated by the provided image. The figure focuses on contrasting the performance of a traditional PID controller whose parameters were tuned manually or via classical methods (usually represented by a dashed red line) against the performance of a PID controller whose parameters have undergone a rigorous optimization process using the Particle Swarm Optimization (PSO) algorithm (typically represented by a solid blue line). This type of visual representation allows the engineer to assess several vital aspects of control system performance directly and immediately firstly, it enables the evaluation of Steady-State Tracking Accuracy, which is the proximity of the system output to the reference value after transient periods have subsided secondly, and most critically in the context of the main title.

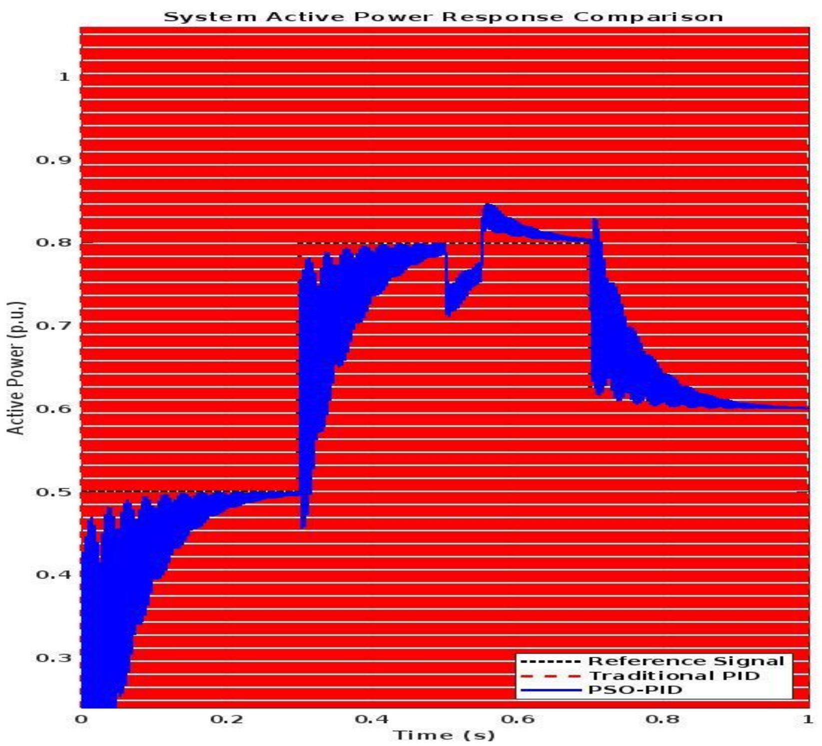

Fig. 8: Comparison of System Active Power Responses

The Transient Response can be analyzed in meticulous detail this includes observing the system's behavior during abrupt and sharp changes in the reference signal (such as the applied step changes) or when the system is subjected to external disturbances. From this one can measure the system's speed of response determine the extent of Overshoot (where the output temporarily exceeds the reference value) monitor the presence and severity of any Oscillations before settling and estimate the overall Settling Time thirdly, although the impact of a disturbance might not be fully evident in this specific image without precise knowledge of its timing and magnitude. This type of plot is fundamentally used to assess the system's Disturbance Rejection capability that is how quickly and effectively the system returns to its stable operating state after being subjected to a disturbance.

The connection of this figure to the code Is established through the variables generated and stored during the various simulation processes. The reference signal (reference signal) is defined in the simulation parameters section and includes the step changes designed to test the system .The system output vector when using the traditional PID controller (trad) is computed and stored in the traditional PID simulation section similarly, the system output vector when using the PSO-optimized PID controller (y_pso) is computed and stored after the completion of the optimization process in the PSO section , subsequently, MATLAB's plotting commands (plot) are utilized to render these time-series vectors against the overall simulation time vector (time vector), producing the superimposed curves that facilitate direct visual comparison.

Upon analyzing the curves presented in the provided image, which appears to suffer from a dense overlay of red lines potentially obscuring the detailed response of the traditional PID. We can focus on the reference signal (dashed black line) and the PSO-PID response (solid blue line) which are more clearly visible. The reference signal distinctly shows the programmed steps at 0.3 seconds and 0.7 seconds. The PSO-PID response however, exhibits complex dynamic behavior at startup and also at each abrupt change in the reference signal. The PSO-PID controller responds rapidly but it displays a noticeable overshoot where the actual power temporarily exceeds the reference value before beginning to settle .Some oscillations are also apparent during these transient periods for instance, during the first step from 0.5 p.u , to 0.8 p.u., the blue line rises above 0.8 p.u , and then oscillates slightly before stabilizing during the presumed disturbance period (between 0.5 and 0.55 seconds in the original code), a sharp, temporary dip in the PSO-PID output is observed reflecting the disturbance's impact on the system followed by the system's attempt to recover and return to the reference value. After each transient period, the PSO-PID controller appears to eventually approach the reference signal, but a precise assessment of steady-state error would require closer examination or numerical data , if we assume that the dense red lines represent a very poor performance of the traditional PID controller or perhaps its instability this indirectly underscores the significant benefit of the PSO optimization process even if the PSO-PID performance still exhibits some shortcomings (such as overshoot and oscillation) it likely represents a substantial improvement over an unoptimized traditional alternative.The comprehensive engineering conclusions derivable from this figure are critical firstly, it affirms the effectiveness of the PSO algorithm in enhancing PID controller performance as the optimized controller demonstrates the ability to track reference changes and respond to disturbances secondly, it highlights the remaining challenges in the PSO-PID's performance, such as the observed overshoot and oscillations which might stem from the resonant nature of the LCL system, the limitations of the cost function used in PSO or the inherent trade-offs between response speed and stability.

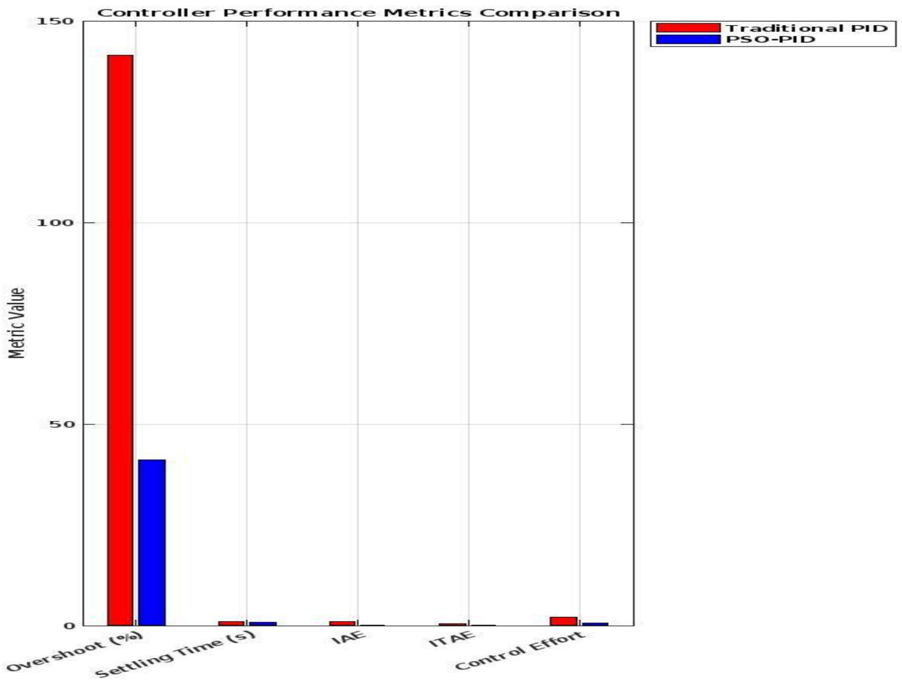

Fig. 9: Comparing Controller Performance Metrics

Figure 7 serves as a powerful and concise tool for the quantitative comparison of the overall performance achieved by the different control strategies implemented: the traditional PID and the PSO-optimized PID it visually presents key performance indices, which are scalar values summarizing complex dynamic behaviors thereby allowing for an objective assessment of which controller performs better according to predefined engineering criteria. The metrics typically included and shown in the provided image are Overshoot (%), Settling Time (s), Integral Absolute Error (IAE), Integral Time-weighted Absolute Error (ITAE), and Control Effort. Each of these metrics captures a different, yet crucial aspect of the control system's quality. The generation of this figure in the MATLAB code relies on the performance trad and performances structures, which are populated at the end of the simulation loops for the traditional PID (Section 3) and the PSO-PID (Section 4), respectively. These structures store the calculated values for each performance index. The bar chart is then created by plotting these values side-by-side for each metric using different colors (red for traditional PID, blue for PSO-PID in the image) to distinguish between the controllers.

Analyzing the provided bar chart, "Controller Performance Metrics Comparison," yields clear and significant engineering insights for the "Overshoot (%)" metric. The red bar (Traditional PID) is exceptionally tall, indicating a very high percentage overshoot so high in fact that it dominates the scale (the value appears to be around 140-145% from the y-axis), in contrast the blue bar (PSO-PID) shows a substantially lower overshoot (around 40-42%). This drastic reduction demonstrates PSO's success in tuning the PID gains to mitigate excessive overshooting, which is crucial for preventing stress on the system and ensuring that the output does not deviate too far from the desired setpoint during transients for "Settling Time (s)," both bars are relatively short but the blue bar (PSO-PID) appears to be slightly shorter or comparable to the red bar (Traditional PID) without exact values it's hard to make a definitive statement but it suggests that PSO while significantly reducing overshoot .Also managed to achieve a competitive or slightly better settling time a fast settling time is critical for systems that need to respond quickly and stabilize after changes or disturbances. The "IAE" and "ITAE" metrics, which quantify the accumulated error over time show a dramatic improvement with the PSO-PID controller. The red bars for the Traditional PID are noticeably taller than the almost negligible blue bars for the PSO-PID, this indicates that the PSO-optimized controller maintains the system output much closer to the reference signal over the entire simulation period, resulting in significantly less cumulative error, lower IAE and ITAE values are direct indicators of superior tracking performance and better overall regulation quality. Figure 10 offers profound visual insight into the distribution of solutions that individual particles within the Particle Swarm Optimization (PSO) algorithm deemed personally optimal (pbest) upon the termination of the optimization process , this distribution is typically rendered in a two-dimensional space representing two of the parameters undergoing optimization; in this specific instance, the Proportional Gain (Kp) is displayed on the horizontal axis and the Integral Gain (Ki) on the vertical axis , a color-coding scheme, elucidated by the adjacent color bar, is employed to denote the cost function value (pbest Cost) associated with each pbest location , furthermore, the globally optimal solution achieved by the entire swarm (Global Best, gbest) is prominently distinguished by a unique marker, such as the purple star in the provided image , from an engineering perspective, this figure furnishes valuable information regarding several facets of the optimization procedure , firstly, it illustrates the extent of convergence or divergence of the particles within the search space , if all pbest points are tightly clustered around the gbest, it signifies that the swarm has converged effectively towards a promising solution region, conversely, a widely scattered distribution of points might indicate a complex search space characterized by numerous local optima, or that the algorithm did not fully converge , secondly, the figure reveals the nature of the "cost surface" within the explored region , a concentration of low-cost points (represented by darker colors in the image) can suggest the presence of a "valley" or a flat region in the cost surface where many good, closely-related solutions exist , thirdly, it aids in assessing the algorithm's efficacy in exploring the parameter space , a well-distributed set of points across reasonable ranges of Kp and Ki implies that the algorithm did not prematurely stagnate in a local optimum .

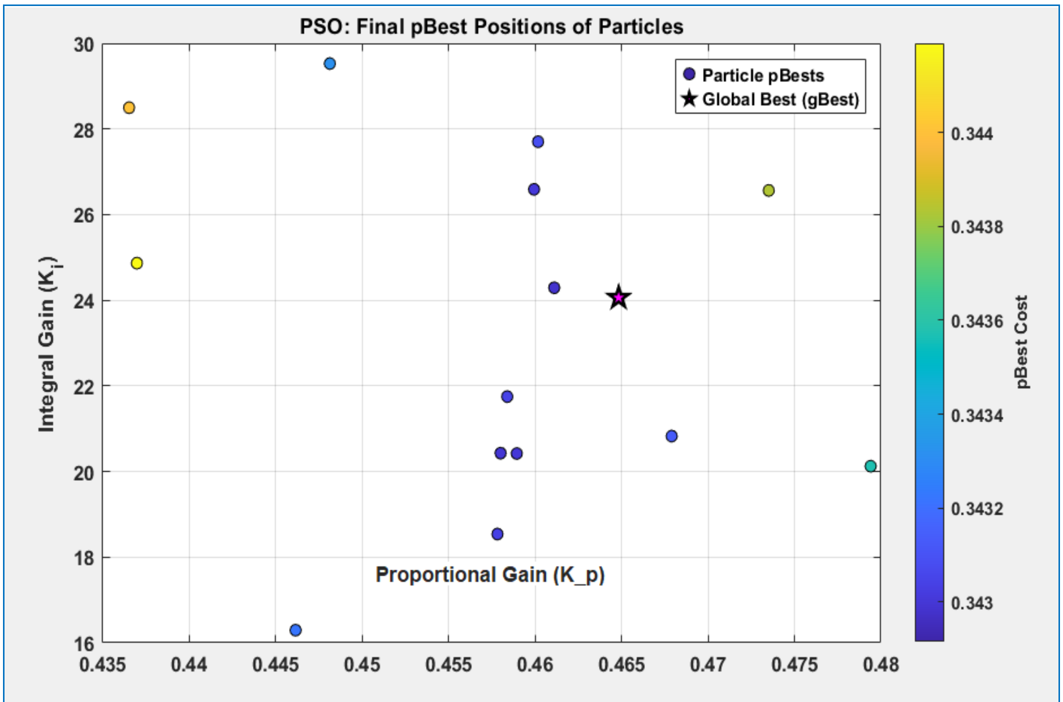

Fig. 10: PSO: Particles' Ultimate Positions

The final personal best positions of the particles are stored in the pbest_pos matrix and their corresponding cost values are stored in p_best_cost_pso_val at the conclusion of the PSO iterations. The displayed figure represents the final state of these variables, p_best_pso (Kp values) are plotted against pbest_pos (Ki values) with p_best_cost_pso_val determining the color of each point. Analyzing the provided image, we observe that the pbest points (diamond-shaped markers) are distributed across a specific range of Kp values (approximately from 0.44 to 0.48) and Ki values (approximately from 16 to nearly 30). The majority of the points with the lowest cost (dark blue and purple colors at the bottom of the color bar, corresponding to cost values around 0.343) are concentrated in a particular region and the global best solution gbest (the purple star) is situated within this cluster, at a Kp of approximately 0.465 and a Ki of about 24. This indicates good convergence of the algorithm towards a region of high-performance solutions. The presence of some pbest points with slightly higher costs (lighter colors such as yellow and light green) in other areas of the search space (e.g., lower Kp with higher Ki, or higher Kp with lower Ki) suggests that the algorithm explored these regions but found the solutions therein to be less optimal .The figure implies the existence of a relatively promising zone where good PID parameters can be found and that the gbest indeed represents the best solution identified within this exploration.

4.1 Discussion

The results of this study which methodically show how Particle Swarm Optimization (PSO) significantly improves PID controller performance for microgrid inverter transient power sharing are in line with a substantial amount of recent research. Studies using PSO for controller tuning in a variety of power system applications have consistently shown that the PSO-PID controller performs better than its traditionally tuned counterpart in terms of minimizing tracking errors, reducing overshoot, and optimizing control effort. While PSO optimizes a given controller structure inherent system characteristics may require more sophisticated strategies beyond simple PID gain tuning this further supports this direction. The effectiveness of PSO is well-documented for various control objectives. Our study contributes by providing a detailed characterization of PSO-PID for inverter-based transient power sharing with an LCL filter identifying both its strengths and limitations concerning system resonances. This demonstrates the general effectiveness of such optimization techniques but a thorough examination also revealed lingering dynamic issues particularly underdamped resonant modes caused by the LCL filter. The trend towards intelligent and adaptive control is evident for managing the growing complexity of contemporary microgrids. The wider context of microgrid control which includes issues like islanding detection and power quality benefits from strong base-level controllers like the PSO-PID developed here prior to the introduction of more complex adaptive layers.

5.Conclusions

This research has systematically investigated and demonstrated the substantial improvements achievable in the control of transient power sharing for a microgrid inverter through the application of Particle Swarm Optimization for PID controller tuning .The PSO-PID demonstrated superior capability in tracking step changes in the power reference and in managing the impact of external disturbances while maintaining its control signal well within practical saturation limits a feat the traditional PID struggled to achieve . The study highlighted the importance of the objective function design in the PSO process the convergence of the g best objective function components demonstrated how the algorithm prioritizes different performance aspects based on their assigned weights, the behavior of the settling time component in particular suggested that the accuracy of performance metric calculation within the optimization loop itself is crucial for effective multi-objective optimization.

Author Contributions: The authors contributed to all parts of the current study.

Funding: This study received no external funding.

Conflicts of Interest: The authors declare no conflict of interest.

Reference

[1] V. N. Ogar, S. Hussain, and K. A. A. Gamage, “Load Frequency Control Using the Particle Swarm Optimisation Algorithm and PID Controller for Effective Monitoring of Transmission Line,” *Energies*, vol. 16, no. 15, 2023, doi: 10.3390/en16155748.

[2] M. Irfan, S. Deilami, S. Huang, T. Tahir, and B. P. Veettil, “Optimizing load frequency control in microgrid with vehicle-to-grid integration in Australia: Based on an enhanced control approach,” *Appl. Energy*, vol. 366, no. May, p. 123317, 2024, doi: 10.1016/j.apenergy.2024.123317.

[3] M. R. Khalghani, S. Khushalani-Solanki, and J. Solanki, “A load frequency control for microgrid including stochastic elements based on Hebb Learning,” *2017 North Am. Power Symp. NAPS 2017*, no. September, pp. 1–7, 2017, doi: 10.1109/NAPS.2017.8107340.

[4] Saleem, M. A. Raza, S. W. Umer, M. Faheem, T. A. Jumani, and M. Yameen, “An Intelligent Frequency Control Scheme for Inverting Station in High Voltage Direct Current Transmission System,” *Eng. Reports*, vol. 7, no. 1, 2025, doi: 10.1002/eng2.13106.

[5] V. Veerasamy *et al.*, “Automatic load frequency control of a multi-area dynamic interconnected power system using a hybrid PSO-GSA-Tuned PID controller,” *Sustain.*, vol. 11, no. 24, 2019, doi: 10.3390/su11246908.

[6] F. Bano, M. Ayaz, D. E. Ze. Baig, and S. M. H. Rizvi, “Intelligent Control Algorithms for Enhanced Frequency Stability in Single and Interconnected Power Systems,” *Electron.*, vol. 13, no. 21, pp. 1–27, 2024, doi: 10.3390/electronics13214219.

[7] A. Daraz, S. Abdullah Malik, I. U. Haq, K. B. Khan, G. F. Laghari, and F. Zafar, *Modified PID controller for automatic generation control of multi-source interconnected power system using fitness dependent optimizer algorithm*, vol. 15, no. 11 November. 2020. doi: 10.1371/journal.pone.0242428.

[8] A. M. Shawqran, M. A. Attia, S. F. Mekhamer, H. Kotb, M. A. Ibrahim, and A. Mordi, “Enhancing Load Frequency Control in Power Systems Using Hybrid PIDA Controllers Optimized with TLBO-TS and TLBO-EDO Techniques,” *Processes*, vol. 13, no. 5, pp. 1–18, 2025, doi: 10.3390/pr13051532.

[9] Z. M. Ali, A. M. Ahmed, H. M. Hasanien, and S. H. E. A. Aleem, “Optimal Design of Fractional-Order PID Controllers for a Nonlinear AWS Wave Energy Converter Using Hybrid Jellyfish Search and Particle Swarm Optimization,” *Fractal Fract.*, vol. 8, no. 1, 2024, doi: 10.3390/fractalfract8010006.

[10] T. D. Raj, C. Kumar, P. Kotsampopoulos, and H. H. Fayek, “Load Frequency Control in Two-Area Multi-Source Power System Using Bald Eagle-Sparrow Search Optimization Tuned PID Controller,” *Energies*, vol. 16, no. 4, 2023, doi: 10.3390/en16042014.

[11] C. Melkia, M. Attia, R. Daouadi, and K. Rais, “Improved PMSM Speed Control Using Backstepping: Stability and Performance Analysis,” *J. Eur. des Syst. Autom.*, vol. 58, no. 2, pp. 383–392, 2025, doi: 10.18280/jesa.580219.

[12] J. Ghasemi, S. M. Rakhtala, J. Rasekhi, and S. R. Dokhtala, “PEM fuel cell system to extend the stack life based on a PID-PSO controller design,” *Complex Eng. Syst.*, vol. 2, no. 1, 2022, doi: 10.20517/ces.2022.02.

[13] J. Mitra, S. B. Patra, and S. J. Ranade, “Reliability stipulated microgrid architecture using particle swarm optimization,” *2006 9th Int. Conf. Probabilistic Methods Appl. to Power Syst. PMAPS*, 2006, doi: 10.1109/PMAPS.2006.360256.

[14] B. Ganthia and K. Rout, “Deregulated Power System Based Study of Agc Using Pid and Fuzzy Logic Controller,” *Int. J. Adv. Res.*, vol. 4, no. 6, pp. 847–855, 2016, doi: 10.21474/ijar01/823.

[15] J. Yang and C. Su, “Robust optimization of microgrid based on renewable distributed power generation and load demand uncertainty,” *Energy*, vol. 223, p. 120043, 2021, doi: 10.1016/j.energy.2021.120043.

[16] S. Nadweh, O. Khaddam, G. Hayeh, B. Atieh, and H. Haes Alhelou, “Steady state analysis of modern industrial variable speed drive systems using controllers adjusted via grey wolf algorithm & particle swarm optimization,” *Heliyon*, vol. 6, no. 11, p. e05438, 2020, doi: 10.1016/j.heliyon.2020.e05438.

[17] G. Ahmad, N. M. Al-yazidi, and M. M. Hamdan, “Metaheuristic-Based Load Frequency Control for EVs-Integrated Hybrid Power Systems with Delays,” *2025 IEEE 22nd Int. Multi-Conference Syst. Signals & Devices*, no. February, pp. 922–927, 2025, doi: 10.1109/SSD64182.2025.10989875.

[18] S. Mahboob Ul Hassan, M. A. M. Ramli, and A. H. Milyani, “Robust Load Frequency Control of Hybrid Solar Power Systems Using Optimization Techniques,” *Front. Energy Res.*, vol. 10, no. July, 2022, doi: 10.3389/fenrg.2022.902776.

[19] L. Ravi, C. V. Kumar, and M. R. Babu, “Stochastic Optimal Management of Renewable Microgrid Using Simplified Particle Swarm Optimization Algorithm,” *Proc. 4th Int. Conf. Electr. Energy Syst. ICEES 2018*, pp. 261–266, 2018, doi: 10.1109/ICEES.2018.8443258.

[20] N. K. Kumar and V. Indragandhi, “Analysis on various optimization techniques used for load frequency control in power system,” *Serbian J. Electr. Eng.*, vol. 15, no. 3, pp. 249–273, 2018, doi: 10.2298/sjee1803249k.